

IN-MEDIUM ω -MESON BROADENING AND S-WAVE
PION ANNIHILATION INTO e^+e^- PAIRS

Gyuri Wolf

CRIP, H-1525 Budapest, Hungary

Bengt Friman

*GSI, Planckstrasse 1
D-64291 Darmstadt, Germany
Institut für Kernphysik, TH Darmstadt
D-64289 Darmstadt, Germany*

and

Madeleine Soyeur

*Département d'Astrophysique, de Physique des Particules,
de Physique Nucléaire et de l'Instrumentation Associée
Service de Physique Nucléaire
Commissariat à l'Energie Atomique/Saclay
F-91191 Gif-sur-Yvette Cedex, France*

Abstract

An ω -meson in motion with respect to a nuclear medium can couple to a σ -meson through a particle-hole excitation. This coupling is large. We investigate its consequences for the width of ω -mesons in matter and for the s-wave annihilation of pions into lepton pairs which can take place in relativistic heavy ion collisions. We find that the two pion decay of ω -mesons, resulting from the $\omega-\sigma$ transition and the subsequent 2π decay of the σ -meson, leads to a substantial broadening of ω -mesons in matter and possibly to an observable effect in experiments measuring the e^+e^- decay of vector mesons produced in nuclei and in relativistic heavy-ion collisions. The inverse process, the s-wave annihilation of pions into ω -mesons decaying into e^+e^- pairs, has in general a much smaller cross section than the corresponding p-wave annihilation through ρ -mesons and is expected to contribute rather little to the total e^+e^- pair production in relativistic heavy ion collisions.

1. Introduction

In general, a meson which interacts with a nuclear medium does not have well-defined quantum numbers as in free space. Both continuous space-time symmetries (such as Lorentz invariance) and discrete symmetries (parity, charge conjugation, G-parity) can be broken. For example, the motion of a meson which propagates with respect to the medium with a 3-momentum $\vec{q} \neq 0$ introduces a spatial direction which breaks rotational invariance and allows for the mixing of meson states of different total angular momenta. To lowest order, this mixing is generated by the coupling of the mesons to particle-hole excitations. We restrict ourselves to symmetric nuclear matter, a situation in which isospin is conserved.

Of particular interest is the mixing of vector and scalar mesons in nuclear matter. In the isovector channel, the ρ -exchange is a major part of the short-range particle-hole interaction which inhibits pion condensation [1]. In the isoscalar channel, the coupling of the σ and ω fields through particle-hole excitations is extremely large and is therefore expected to strongly affect the propagation of ω -mesons in nuclear matter [2,3].

In view of the role that vector mesons play both in hadronic physics and in nuclear dynamics, the propagation of ρ - and ω -mesons in matter is at present the subject of many theoretical investigations. These studies have been largely motivated by the suggestion that in-medium vector meson masses could be order parameters for chiral symmetry restoration at large baryon density [4]. In this case, the masses of the ρ - and ω -mesons would decrease with increasing density as a consequence of their close relation to the quark condensate. To test this idea, measurements of the e^+e^- spectrum of vector mesons produced in nuclei and in heavy ion collisions are planned at TJNAF [5] and GSI [6]. The kinematics is chosen so that at least ρ -mesons decay inside the nuclear medium. We recall that the $\rho(770)$ and $\omega(782)$ have similar masses but very different widths, $\Gamma_\rho = (151.2 \pm 1.2)$ MeV and $\Gamma_\omega = (8.43 \pm 0.10)$ MeV, corresponding to propagation lengths of $c\tau_\rho = 1.3$ fm and $c\tau_\omega = 23.4$ fm in free space [7]. The e^+e^- spectrum will reflect the spectral function of vector meson-like excitations in matter. At sufficiently low density and temperature, it is expected that these excitations will behave as quasi-particles which can be characterized by a mass and a width.

The in-medium width of ρ - and ω -mesons plays a major role in the observability of their in-medium mass. The in-medium widths of vector mesons determine their mean free path in matter and the probability that they decay inside the nuclear target (or in the interaction region for heavy ion collisions) after they are produced. In this respect, the medium broadening of the ω -meson is particularly important because it could make its lifetime comparable to the size of the nuclear system in which it is produced.

The dynamical broadening of ω -mesons in matter can come from elastic and inelastic processes [8]. Collisional broadening is expected in particular from the $\omega N \rightarrow \pi N$ reaction which has a fairly large cross section and can cause a significant absorption of ω -mesons into the pion channel. By applying detailed balance we find, using the measured $\pi N \rightarrow \omega N$ cross section [9], a contribution to the ω width in matter of ≈ 10 MeV at normal nuclear density [10]. The $\omega N \rightarrow \rho N$ reaction can also play a role and lead to the absorption of ω -mesons into

the p-wave two-pion channel. In this paper, we work out the additional width of ω -mesons in matter arising from the large $\omega\sigma$ mixing in matter. The σ meson is an effective degree of freedom which parametrizes the propagation of two pions in s-wave. The coupling of the ω to the σ in matter opens therefore a new two pion decay channel for the ω -meson. We show that the associated broadening of the ω -meson is large and increases with baryon density as well as with the momentum of the ω -meson. Conversely, the in-medium coupling of the σ to the ω makes it possible for two pions in s-wave to annihilate into a lepton pair through an intermediate ω -meson [11,12]. We discuss the consequences of this new annihilation channel for the production of e^+e^- pairs in relativistic heavy ion collisions.

In Section 2, we compute the $\omega\sigma$ polarization at finite density and temperature in the one-loop approximation. The $\sigma\pi\pi$ coupling constant and the σ mass are fitted to the $\pi\pi$ s-wave scattering phase shifts in Section 3. Our numerical results for the in-medium ω broadening and s-wave pion annihilation into e^+e^- pairs are discussed in Section 4 and we conclude with a brief discussion in Section 5.

2. Calculation of the $\omega\sigma$ polarization

The polarization operator describing the mixing of ω - and σ -mesons to lowest order in matter is shown in Fig. 1. At sufficiently low temperatures, it is dominated by intermediate nucleon-hole states. The two processes discussed in this paper, the broadening of the ω -meson and the s-wave annihilation of pions at finite baryon density and temperature, are directly linked to the polarization operator, as indicated by the diagrams of Fig. 2.

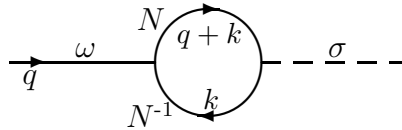


Fig. 1. The $\omega\sigma$ polarisation in nuclear matter.

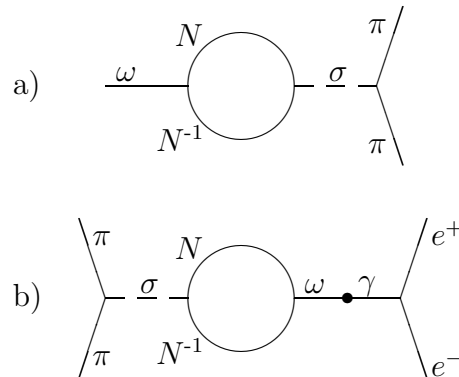


Fig. 2. In-medium $\omega\sigma$ mixing contributions to the ω -meson width (a) and to the s-wave $\pi\pi \rightarrow e^+e^-$ process (b).

We calculate the polarization operator of Fig. 1 in the relativistic mean-field approximation. Nuclear matter is treated as a system of noninteracting fermions at finite density and temperature. We use free space meson fields. The σ - and ω -meson fields couple to the scalar baryon density and to the conserved baryon current respectively,

$$\mathcal{L}_{\sigma NN} = g_\sigma \bar{\Psi} \sigma \Psi \quad (1)$$

and

$$\mathcal{L}_{\omega NN} = -g_\omega \bar{\Psi} \gamma_\mu \omega^\mu \Psi. \quad (2)$$

The $\omega\sigma$ polarization at finite density and temperature is evaluated in the rest frame of nuclear matter. We generalize methods used previously [2,13,14] in calculations restricted to matter at zero temperature. The polarization tensor for the process shown in Fig. 1 is given by the expression,

$$-i\Pi^\mu = -2 g_\sigma g_\omega \int \frac{d^4 k}{(2\pi)^4} \text{Tr}[\gamma^\mu iG(k+q) iG(k)], \quad (3)$$

where $iG(k)$ is the propagator of a nucleon in nuclear matter at finite temperature. The minus sign arises from the fermion loop and the factor of 2 is the isospin degeneracy factor for symmetric nuclear matter. The nucleon propagator can be written as the sum of two terms,

$$iG(k) = iG_0(k) + iG_M(k), \quad (4)$$

the free propagator $iG_0(k)$ and a medium term $iG_M(k)$. At zero temperature, the latter allows for the propagation of holes in the Fermi sea and restricts particle propagation to states above the Fermi surface.

In the mean-field approximation, and neglecting the contribution of thermally excited antibaryons, the nucleon propagator reads

$$iG(k) = i(k + M_N^*) \left\{ \frac{1}{k^2 - M_N^{*2} + i\epsilon} + \frac{i\pi}{E^*(k)} \delta[k^0 - E^*(k)] n_T(k) \right\}, \quad (5)$$

where we have introduced the nucleon effective mass M_N^* , the effective kinetic energy $E^*(k) = (\vec{k}^2 + M_N^{*2})^{1/2}$ and the nucleon thermal distribution function $n_T(k)$

$$n_T(k) = \frac{1}{1 + \exp\{[E^*(k) - \mu]/k_B T\}}. \quad (6)$$

In Eq. (6), μ is the baryon chemical potential and k_B the Boltzmann constant. At zero

temperature, the thermal distribution function $n_T(k)$ is replaced by the step function $\theta(k_F - |\vec{k}|)$.

Evaluating the trace, we have

$$-i\Pi^\mu = 8 M_N^* g_\sigma g_\omega \int \frac{d^4 k}{(2\pi)^4} (2k + q)^\mu \left\{ \frac{1}{k^2 - M_N^{*2} + i\epsilon} + \frac{i\pi}{E^*(k)} \delta[k^0 - E^*(k)] n_T(k) \right\} \\ \left\{ \frac{1}{(k + q)^2 - M_N^{*2} + i\epsilon} + \frac{i\pi}{E^*(k + q)} \delta[k^0 + q^0 - E^*(k + q)] n_T(k + q) \right\}. \quad (7)$$

We need Π^μ only for time-like values of q^2 . The product of the propagators gives four terms. The first one is the vacuum polarization which is zero. The product of the matter terms vanishes for time-like q^2 as the constraints from the δ -functions, $\delta[k^0 - E^*(k)]$ and $\delta[k^0 + q^0 - E^*(k + q)]$, are in this case incompatible. We are left with the two terms linear in n_T , which are free of divergences.

The polarization Π^μ satisfies

$$q_\mu \Pi^\mu = 0, \quad (8)$$

as the ω -field is coupled to a conserved current. We choose a coordinate system such that \vec{q} is along the z axis, i.e. $q_\mu = (q_0, 0, 0, q_z)$. The x and y components of the polarization vanish in this frame due to the axial symmetry. Furthermore, Eq. (8) implies

$$q_0 \Pi_0 = q_z \Pi_z, \quad (9)$$

i.e. there is only one independent component in the polarization tensor. We calculate Π^0 . After integration over k^0 and a change of variable $\vec{k} \rightarrow \vec{k} + \vec{q}$ in the second term, we obtain

$$\Pi^0 = 8 M_N^* g_\sigma g_\omega \int \frac{d^3 \vec{k}}{(2\pi)^3} \left\{ \frac{1}{2E^*(k)} \frac{2E^*(k) + q^0}{E^*(k + q)^2 - [E^*(k) + q^0]^2 - i\epsilon} n_T(k) \right. \\ \left. + \frac{1}{2E^*(k)} \frac{2E^*(k) - q^0}{E^*(k - q)^2 - [E^*(k) - q^0]^2 - i\epsilon} n_T(k) \right\} \quad (10)$$

$$\equiv \Pi_1^0 + \Pi_2^0. \quad (11)$$

Clearly, Π^0 is invariant separately under $q_0 \rightarrow -q_0$ and $\vec{q} \rightarrow -\vec{q}$, while Π_z is odd under those transformations. It is then sufficient to consider $q_0 > 0$. In general, the polarization tensor in matter is a function of \vec{q} as well as of q_0 .

The angular integrals in Eq. (10) are readily performed. We find

$$\Re \Pi_1^0 = \frac{M_N^* g_\sigma g_\omega}{2\pi^2 q_z} \int k dk \frac{2E^*(k) + q^0}{E^*(k)} \ln \frac{q^2 + 2E^*(k)q^0 - 2kq_z}{q^2 + 2E^*(k)q^0 + 2kq_z} n_T(k), \quad (12)$$

$$\Im \Pi_1^0 = 0. \quad (13)$$

for $q^2 > 0$ and $q^0 > 0$.

For Π_2^0 , there are two cases. For $q_0 > 0$ and $0 < q^2 < 4M_N^{*2}$, we have

$$\Re \Pi_2^0 = \frac{M_N^* g_\sigma g_\omega}{2\pi^2 q_z} \int k dk \frac{2E^*(k) - q^0}{E^*(k)} \ln \frac{q^2 - 2E^*(k)q^0 - 2kq_z}{q^2 - 2E^*(k)q^0 + 2kq_z} n_T(k), \quad (14)$$

$$\Im \Pi_2^0 = 0. \quad (15)$$

For $q^2 > 4M_N^{*2}$, the real part reads

$$\Re \Pi_2^0 = \frac{M_N^* g_\sigma g_\omega}{2\pi^2 q_z} \int k dk \frac{2E^*(k) - q^0}{E^*(k)} \ln \left| \frac{q^2 - 2E^*(k)q^0 - 2kq_z}{q^2 - 2E^*(k)q^0 + 2kq_z} \right| n_T(k) \quad (16)$$

and the imaginary part is given by

$$\begin{aligned} \Im \Pi_2^0 = \frac{M_N^* g_\sigma g_\omega}{2\pi q_z} \int k dk \frac{2E^*(k) - q^0}{E^*(k)} \Theta \left[\left(\frac{q_z}{2} + \frac{q^0}{2} \sqrt{1 - \frac{4M_N^{*2}}{q^2}} \right) - k \right] \\ \Theta \left[k - \left(\frac{q_z}{2} - \frac{q^0}{2} \sqrt{1 - \frac{4M_N^{*2}}{q^2}} \right) \right] n_T(k) \end{aligned} \quad (17)$$

for $q^2 < 2q^0 M_N^*$ and by

$$\begin{aligned} \Im \Pi_2^0 = \frac{M_N^* g_\sigma g_\omega}{2\pi q_z} \int k dk \frac{2E^*(k) - q^0}{E^*(k)} \Theta \left[\left(\frac{q_z}{2} + \frac{q^0}{2} \sqrt{1 - \frac{4M_N^{*2}}{q^2}} \right) - k \right] \\ \Theta \left[k + \left(\frac{q_z}{2} - \frac{q^0}{2} \sqrt{1 - \frac{4M_N^{*2}}{q^2}} \right) \right] n_T(k) \end{aligned} \quad (18)$$

for $q^2 > 2q^0 M_N^*$.

The $\omega\sigma$ mixing matrix elements depend on the σNN and ωNN coupling constants, g_σ and g_ω , and on the nucleon effective mass, $M_N^*(\rho)$.

We choose $g_\sigma=12.78$ from Ref. [15]. There is some uncertainty in this quantity linked to the nature of the σ field. The Walecka Model [16] and the One-Boson-Exchange potentials [17] favor somewhat smaller values, on the order of $g_\sigma=10$.

For the ωNN coupling constant, we adopt $g_\omega=9$ as required by universality [18]. We expect this value to be the most adequate one for describing the coupling of physical ω -mesons to nucleons. In the Walecka Model, the preferred value is $g_\omega=11.7$ [16] while an even larger coupling constant $g_\omega \simeq 17$ is used in One-Boson-Exchange potentials [17]. It is likely that various other contributions to the repulsive part of the nucleon-nucleon interaction are subsumed in the effective ω degree of freedom in these approaches.

To calculate the diagrams displayed in Fig. 2, we shall evaluate the polarization at $q^2 = m_\omega^2$. We note that, for $q^2 = m_\omega^2$, a form factor of the form $[(\Lambda^2 - m_\omega^2)/(\Lambda^2 - q^2)]^n$ at the ωNN vertex is strictly equal to unity. Similarly, a form factor of the same form at the σNN vertex, but with m_ω replaced by m_σ , is very close to unity for the same value of q^2 and for $m_\sigma=0.84$ GeV (see below). Consequently, such form factors can be neglected in our calculation.

The density dependence of the nucleon effective mass is determined within the nonlinear field theoretical approach of Ref. [19]. The Lagrangian of this model is obtained by adding nonlinear terms of the form,

$$\mathcal{L}^{NL} = -\frac{aM_N}{3}g_\sigma^3\sigma^3 - \frac{b}{4}g_\sigma^4\sigma^4, \quad (19)$$

to the Walecka scalar-vector model [16]. The parameters of the Lagrangian are fitted to give a reasonable description of the properties of nuclear matter. We impose as constraints the saturation density ($\rho_0 = 0.17 \text{ fm}^{-3}$), the binding energy per nucleon ($E/A=-16 \text{ MeV}$) and the compression modulus ($K=300 \text{ MeV}$). We note that this model allows for values of K much closer to the empirical value than the very large incompressibility ($K\simeq 550 \text{ MeV}$) obtained in the original Walecka model [16]. Furthermore, we fix the nucleon effective mass at saturation density to be $M_N^*(\rho_0) = 0.7 M_N$, a value appropriate for particle-hole excitations involving momenta far above the Fermi surface [20]. However, since our results are very sensitive to the value of the nucleon effective mass, we also give some results obtained with $M_N^*(\rho_0) = 0.8 M_N$. The four parameters of the model are $C_\sigma^2 = g_\sigma^2(M_N/m_\sigma)^2$, $C_\omega^2 = g_\omega^2(M_N/m_\omega)^2$, $A = aM_Ng_\sigma^3$ and $B = bg_\sigma^4$. Their numerical values are $C_\sigma^2 = 243.22$, $C_\omega^2 = 145.77$, $a = 0.321 \cdot 10^{-2}$ and $b = -0.129 \cdot 10^{-2}$ for $M_N^*(\rho_0) = 0.7 M_N$ and $C_\sigma^2 = 173.35$, $C_\omega^2 = 85.82$, $a = 0.256 \cdot 10^{-2}$ and $b = 0.309 \cdot 10^{-1}$ for $M_N^*(\rho_0) = 0.8 M_N$.

3. $\pi\pi$ scattering phase shifts in the s-wave

We present in this section a model for $\pi\pi$ scattering in the s-wave and fix the $\sigma\pi\pi$ vertex (coupling constant and form factor in the time-like region) as well as the σ -meson mass, needed to calculate the processes illustrated in Fig. 2.

We assume that s-wave $\pi\pi$ scattering is dominated by the σ -meson in the s-channel and we compute the σ self-energy to the one-loop order, including both pion and kaon loops, as shown in Fig. 3. We remark that this approach is very different from meson-exchange models in which a potential for $\pi\pi$ scattering is generated by summing the lowest-lying s-, t- and

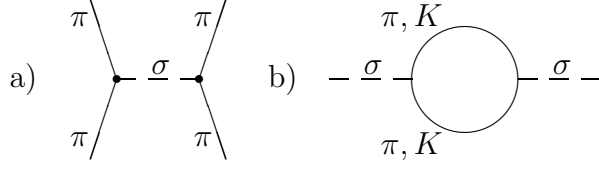


Fig. 3. $\pi\pi$ s-wave scattering (a) and σ self-energy (b).

u-channel exchange diagrams [21].

In resonant scattering, the phase shift is directly related to the resonance propagator. In our model of s-wave $\pi\pi$ scattering, the phase shift δ_0 below the $K\bar{K}$ threshold can be expressed as a function of the real and imaginary parts of the σ -meson propagator G_σ ,

$$\tan(\delta_0(q)) = \frac{\Im m G_\sigma(q)}{\Re G_\sigma(q)} = -\frac{\Im m G_\sigma^{-1}(q)}{\Re G_\sigma^{-1}(q)}, \quad (20)$$

where G_σ is defined by

$$G_\sigma(q) = \frac{1}{q^2 - m_\sigma^0{}^2 - \Sigma(q)}. \quad (21)$$

In Eq. (21), m_σ^0 is the bare σ -meson mass and $\Sigma(q)$ the self-energy associated with the π and K loops of Fig. 3b.

In order to calculate $\Sigma(q)$, we assume the following forms of the interaction Lagrangians

$$\mathcal{L}_{\sigma\pi\pi} = \frac{1}{2} g_{\sigma\pi\pi} m_\pi \vec{\pi} \vec{\pi} \sigma \quad (22)$$

and

$$\mathcal{L}_{\sigma KK} = g_{\sigma KK} m_K (\bar{K}^0 K^0 \sigma + K^+ K^- \sigma). \quad (23)$$

We use extended $\sigma\pi\pi$ and σKK vertices characterized by the same functional form and cutoff,

$$F(q) = \frac{\Lambda^2}{\Lambda^2 - q^2}. \quad (24)$$

The form factor effectively accounts for higher order processes, not included in the lowest order approximation.

The self-energy $\Sigma(q)$ is given by

$$\begin{aligned}
-i\Sigma(q) = & \frac{3}{2} g_{\sigma\pi\pi}^2 m_\pi^2 F^2(q^2) \int \frac{d^4 k_1}{(2\pi)^4} \frac{1}{k_1^2 - m_\pi^2 + i\epsilon} \frac{1}{(k_1 - q)^2 - m_\pi^2 + i\epsilon} \\
& + 2 g_{\sigma KK}^2 m_K^2 F^2(q^2) \int \frac{d^4 k_2}{(2\pi)^4} \frac{1}{k_2^2 - m_K^2 + i\epsilon} \frac{1}{(k_2 - q)^2 - m_K^2 + i\epsilon}, \quad (25)
\end{aligned}$$

where the coefficient $3/2$ for the pion loop comes from the the 3 isospin states and the permutation symmetry factor and the coefficient 2 for the kaon loop accounts for the neutral and charged kaon contributions. We are interested in fitting the s-wave $\pi\pi$ phase shifts for values of \sqrt{s} of the order of the ω -meson mass, i.e. typically between $\sqrt{s} = 2m_\pi$ and $\sqrt{s} = 2m_K$. In this range, $4m_\pi^2 < q^2 < 4m_K^2$, the contribution of the pion loop to $\Sigma(q)$ has both real and imaginary parts while the contribution of the kaon loop is real.

The pion and kaon loops are logarithmically divergent. We regularize the corresponding integrals using the Pauli-Villars method [22]. We couple for each loop the σ -meson to an additional pseudoscalar field with a very large mass and multiply the regularizing integrals by constants chosen so as to remove the divergences. This procedure is discussed in detail for the calculation of the vacuum polarization in quantum electrodynamics in Ref. [23].

For $4m_\pi^2 < q^2 < 4m_K^2$, we find

$$\begin{aligned}
\Re \Sigma(q) = & -\frac{3}{16\pi^2} g_{\sigma\pi\pi}^2 m_\pi^2 F^2(q^2) \left\{ \ln \frac{m_\Lambda}{m_\pi} + \frac{1}{2} \left(\frac{q^2 - 4m_\pi^2}{q^2} \right)^{1/2} \ln \left[\frac{q - (q^2 - 4m_\pi^2)^{1/2}}{q + (q^2 - 4m_\pi^2)^{1/2}} \right] \right. \\
& \left. - \frac{1}{2} \left(\frac{4m_\Lambda^2 - q^2}{q^2} \right)^{1/2} \left[2 \arctan \left(\frac{4m_\Lambda^2 - q^2}{q^2} \right)^{1/2} - \pi \right] \right\} \\
& - \frac{1}{4\pi^2} g_{\sigma KK}^2 m_K^2 F^2(q^2) \left\{ \ln \frac{m_{\Lambda'}}{m_K} \right. \\
& + \frac{1}{2} \left(\frac{4m_K^2 - q^2}{q^2} \right)^{1/2} \left[2 \arctan \left(\frac{4m_K^2 - q^2}{q^2} \right)^{1/2} - \pi \right] \\
& \left. - \frac{1}{2} \left(\frac{4m_{\Lambda'}^2 - q^2}{q^2} \right)^{1/2} \left[2 \arctan \left(\frac{4m_{\Lambda'}^2 - q^2}{q^2} \right)^{1/2} - \pi \right] \right\} \quad (26)
\end{aligned}$$

and

$$\Im \Sigma(q) = -\frac{3}{32\pi} g_{\sigma\pi\pi}^2 m_\pi^2 F^2(q^2) \left(\frac{q^2 - 4m_\pi^2}{q^2} \right)^{1/2}, \quad (27)$$

where m_Λ and $m_{\Lambda'}$ are the Pauli-Villars masses and $q = \sqrt{q^2}$. The value of the physical mass of the σ -meson in our model is fixed by the condition

$$\Re G_\sigma^{-1}(q^2 = m_\sigma^2) = 0. \quad (28)$$

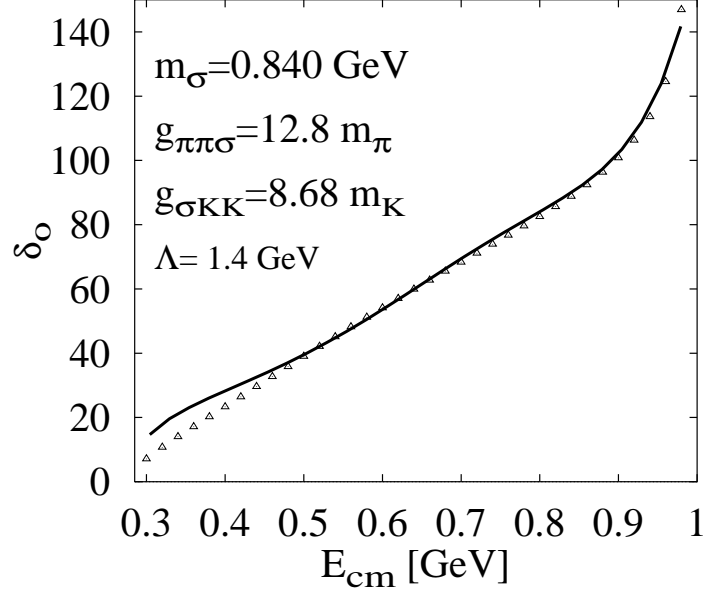


Fig. 4. Fit to the $\pi\pi$ s-wave scattering phase shift.

This relation provides the functional dependence of $m_\sigma^{0,2}$ on m_σ^2 . Inserting this value of $m_\sigma^{0,2}$ in the expression for $G_\sigma(q)$, we obtain

$$\Re G_\sigma^{-1}(q^2) = q^2 - m_\sigma^2 - (\Sigma(q^2) - \Sigma(m_\sigma^2)). \quad (29)$$

For m_Λ and $m_{\Lambda'}$ approaching infinity, the terms involving the Pauli-Villars masses vanish and the physical contribution to $\Re G_\sigma^{-1}(q^2)$ is given by the remaining terms,

$$\begin{aligned} \Re G_\sigma^{-1}(q^2) = & q^2 - m_\sigma^2 \\ & - \frac{3}{16\pi^2} g_{\sigma\pi\pi}^2 m_\pi^2 \left\{ F^2(m_\sigma^2) \left(\frac{m_\sigma^2 - 4m_\pi^2}{4m_\sigma^2} \right)^{1/2} \ln \left[\frac{m_\sigma - (m_\sigma^2 - 4m_\pi^2)^{1/2}}{m_\sigma + (m_\sigma^2 - 4m_\pi^2)^{1/2}} \right] \right. \\ & \left. - F^2(q^2) \left(\frac{q^2 - 4m_\pi^2}{4q^2} \right)^{1/2} \ln \left[\frac{q - (q^2 - 4m_\pi^2)^{1/2}}{q + (q^2 - 4m_\pi^2)^{1/2}} \right] \right\} \\ & - \frac{1}{4\pi^2} g_{\sigma KK}^2 m_K^2 \left\{ F^2(m_\sigma^2) \left(\frac{4m_K^2 - m_\sigma^2}{4m_\sigma^2} \right)^{1/2} \left[2 \arctan \left(\frac{4m_K^2 - m_\sigma^2}{m_\sigma^2} \right)^{1/2} - \pi \right] \right. \\ & \left. - F^2(q^2) \left(\frac{4m_K^2 - q^2}{4q^2} \right)^{1/2} \left[2 \arctan \left(\frac{4m_K^2 - q^2}{q^2} \right)^{1/2} - \pi \right] \right\} \end{aligned} \quad (30)$$

and

$$\Im G_\sigma^{-1}(q^2) = \frac{3}{32\pi} g_{\sigma\pi\pi}^2 m_\pi^2 F^2(q^2) \left(\frac{q^2 - 4m_\pi^2}{q^2} \right)^{1/2}. \quad (31)$$

Using Eq. (20), we can fit the s-wave $\pi\pi$ phase shift δ_0 . The result, displayed in Fig. 4,

is obtained with $m_\sigma=0.84$ GeV, $g_{\sigma\pi\pi}=12.8$, $g_{\sigma KK}=8.68$ and $\Lambda=1.4$ GeV. Considering the complexity of the σ degree of freedom and the simplicity of the model, this fit is remarkably good. It is particularly precise in the region of interest for our problem, i.e. around $\sqrt{s} \simeq m_\omega$.

4. Numerical results

4.1. In-medium broadening of ω -mesons of finite momenta

In this subsection, we calculate the process illustrated in Fig. 2a. We consider an ω -meson on its mass-shell ($q^2 = m_\omega^2, q_z \neq 0$) which converts into a σ -meson through a particle-hole excitation and decays into two pions of momenta k_1 and k_2 respectively.

In the nuclear matter rest frame, the partial decay width for this process is given by [23]

$$\Gamma_{\omega \rightarrow \pi\pi} = \frac{1}{24\pi^2 q^0} \frac{3}{2} \int \frac{d^3 k_1}{2k_1^0} \frac{d^3 k_2}{2k_2^0} \sum_{spins} |M|^2 \delta^4(q - k_1 - k_2), \quad (32)$$

where M is the invariant transition matrix element and the factor $3/2$ accounts for the sum over isospin and the symmetry of the final state.

Using the interaction Lagrangian (22) and the results of Section 2, a straightforward calculation yields

$$\Gamma_{\omega \rightarrow \pi\pi} = \frac{(g_{\sigma\pi\pi} m_\pi)^2}{4\pi} F^2(q^2 = m_\omega^2) \frac{k_\pi}{4q_z^2} \frac{m_\omega}{q^0} |G_\sigma(q^2 = m_\omega^2)|^2 [\Pi^0(q^2 = m_\omega^2, q_z)]^2, \quad (33)$$

where the form factor F is defined by Eq. (24), $k_\pi = \sqrt{m_\omega^2/4 - m_\pi^2}$ is the pion 3-momentum in the ω rest frame, G_σ and Π^0 are the σ propagator [Eqs. (30) and (31)] and the $\omega\sigma$ polarization [Eqs. 12-18] respectively.

In Figs. 5-7, we show $\Gamma_{\omega \rightarrow \pi\pi}$ as a function of density, ω -meson 3-momentum and temperature. In each figure, we indicate also the free ω width which should be added to the matter contribution (33).

We discuss first the ω broadening due to the $\omega\sigma$ polarization in nuclear matter at zero temperature (Fig. 5). The most striking result is that $\Gamma_{\omega \rightarrow \pi\pi}$ is very large. At $\rho = \rho_0$, $\Gamma_{\omega \rightarrow \pi\pi}$ is 27 MeV for $q_z=0.5$ GeV/c, i.e. in the momentum range where the broadening is most pronounced. The reason for this is twofold. On the one hand, as already noted in Ref. [2], the $\omega\sigma$ polarization is large. On the other hand, the σ propagator taken at $q^2 = m_\omega^2$ enhances the effect. Its real part is indeed very small since our value for m_σ is close to m_ω [$m_\omega^2 - m_\sigma^2 = -0.094$ GeV²]. Furthermore, $\Gamma_{\omega \rightarrow \pi\pi}$ is also very sensitive to the nucleon effective mass. We illustrate this effect in Fig. 5 by showing the values of $\Gamma_{\omega \rightarrow \pi\pi}$ obtained for $M_N^*(\rho_0) = 0.8 M_N$. With this choice for M_N^* , $\Gamma_{\omega \rightarrow \pi\pi}$ is reduced by about 8 MeV at $\rho = \rho_0$. The

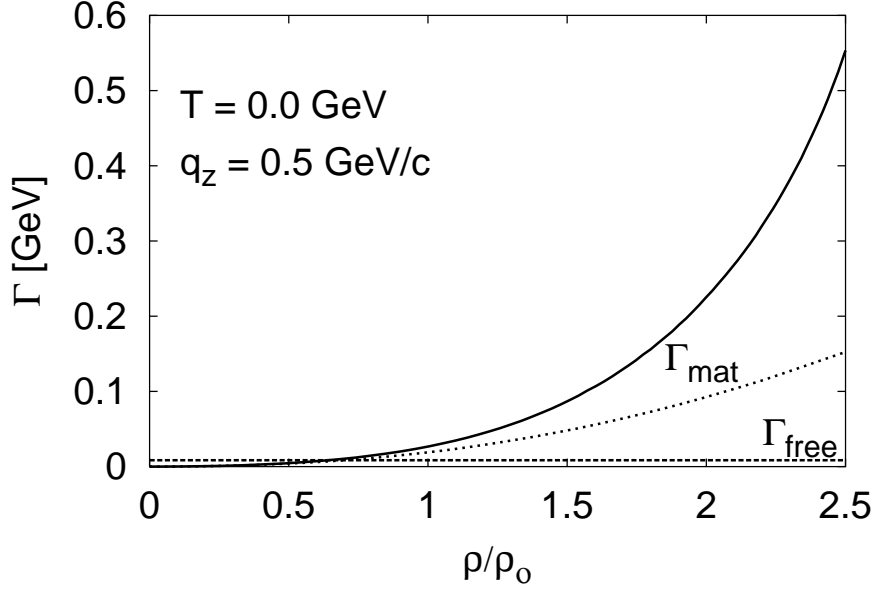


Fig. 5. Density dependence of $\Gamma_{\omega \rightarrow \pi\pi}$ (denoted Γ_{mat}) at $T=0$ and for an ω 3-momentum $q_z = 0.5$ GeV/c. The full curve is the result obtained with $M_N^*(\rho_0) = 0.7 M_N$; the dotted line shows the effect of using $M_N^*(\rho_0) = 0.8 M_N$ instead. Γ_{free} is the ω width in free space (dashed line).

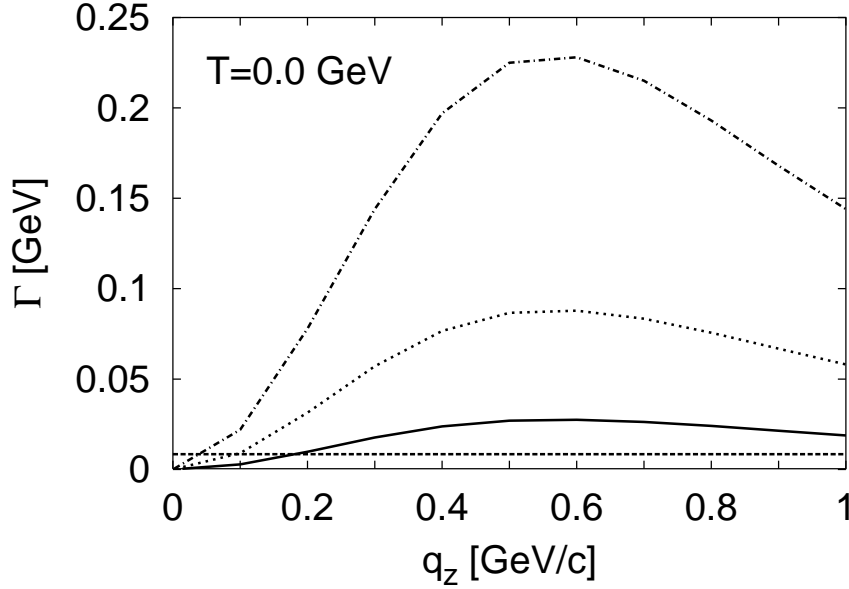


Fig. 6. Momentum dependence of $\Gamma_{\omega \rightarrow \pi\pi}$ at $T=0$ and for 3 values of the matter density $\rho/\rho_0 = 1$ (full line), 1.5 (dotted line) and 2 (dot-dashed line). The free width is indicated by a dashed line.

sensitivity of $\Gamma_{\omega \rightarrow \pi\pi}$ to the density dependence of the nucleon effective mass is very strong at larger densities, where our estimate is therefore much more uncertain than at $\rho = \rho_0$. We note that, in the range of densities considered in Fig. 5, the $\omega\sigma$ polarization is real because $q^2 = m_\omega^2$ is always $< 4M_N^{*2}$. Hence, the in-medium width is due solely to the two-pion final state. As expected, $\Gamma_{\omega \rightarrow \pi\pi}$ exhibits a strong dependence on the baryon density.

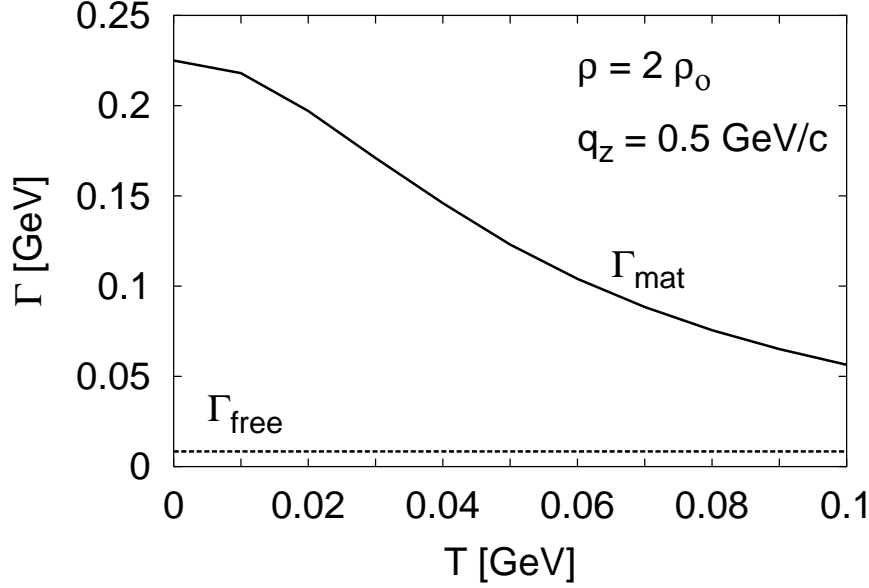


Fig. 7. Temperature dependence of $\Gamma_{\omega \rightarrow \pi\pi}$ (denoted Γ_{mat}) at $q_z = 0.5$ GeV/c and for $\rho/\rho_0 = 2$ (full line). Γ_{free} is the ω width in free space (dashed line).

The 3-momentum dependence of $\Gamma_{\omega \rightarrow \pi\pi}$, displayed in Fig. 6 at $T=0$ for $\rho/\rho_0=1, 1.5$ and 2 , illustrates the kinematic conditions under which the broadening of the ω -meson due to the $\omega\sigma$ polarization is the largest. At $q_z = 0$, where the $\omega\sigma$ mixing is not allowed, $\Gamma_{\omega \rightarrow \pi\pi}$ vanishes. As a consequence of the kinematic factors in Eq. (33), the initial growth of $\Gamma_{\omega \rightarrow \pi\pi}$ with q_z saturates, and is reversed for $q_z > 0.6$ GeV/c.

In Fig. 7, we show the temperature dependence of $\Gamma_{\omega \rightarrow \pi\pi}$ for $\rho/\rho_0=2$ and $q_z = 0.5$ GeV/c. The in-medium ω width due to $\omega\sigma$ mixing decreases with increasing temperature. This effect can be traced back to the temperature dependence of the nucleon effective mass, which increases with increasing temperature in Walecka models. For the temperatures expected to prevail in relativistic heavy ions collisions ($E/A \simeq 1-2$ GeV), $\Gamma_{\omega \rightarrow \pi\pi}$ is decreased by at least a factor of two compared to the $T=0$ value at the same density. We emphasize that this behavior is very much model dependent. The increase of the nucleon effective mass with increasing temperature at finite density ($T < 100$ MeV) is a particular feature of the Walecka model. In models where the nucleon effective mass decreases with increasing temperature, $\Gamma_{\omega \rightarrow \pi\pi}$ would increase with increasing temperature.

4.2. S-wave $\pi\pi$ annihilation into e^+e^- pairs

We discuss now the process illustrated in Fig. 2b and study its importance in the production of e^+e^- pairs in relativistic heavy ion collisions.

We calculate the s-wave annihilation of two pions ($\pi^+\pi^-$ or $\pi^0\pi^0$) of momenta p_1 and p_2 such that $(p_1 + p_2)^2 = m_\omega^2$. They annihilate in the σ channel which, through particle-hole excitations, mixes with the ω -meson. The ω can decay into an electron and a positron of

momenta k_1 and k_2 . The diagram of Fig. 2b is evaluated in the rest frame of the nuclear medium (which we identify with the interaction region in central heavy ion collisions). For each initial state ($\pi^+\pi^-$, $\pi^-\pi^+$ and $\pi^0\pi^0$), the annihilation cross section is given by

$$\sigma_{\pi\pi\rightarrow e^+e^-}^{s-wave} = \frac{1}{8\pi^2 m_\omega} \frac{m_e^2}{\sqrt{m_\omega^2 - 4m_\pi^2}} \int \frac{d^3 k_1}{k_1^0} \frac{d^3 k_2}{k_2^0} \sum_{spins} |M|^2 \delta^4(p_1 + p_2 - k_1 - k_2). \quad (34)$$

The calculation of this cross section involves the same quantities as the partial decay width of Eq. (33). We use the additional assumption of vector meson dominance for the electromagnetic current [24]. The conversion of an ω -meson into a massive photon is characterized by the coupling constant

$$f_\omega = \frac{em_\omega^2}{2g_\omega}. \quad (35)$$

with g_ω defined as in Eq. (2). Neglecting the electron mass compared to the electron momentum, we obtain for the annihilation cross section

$$\begin{aligned} \sigma_{\pi\pi\rightarrow e^+e^-}^{s-wave} = & \frac{\pi}{3q_z^2} \frac{1}{\sqrt{q^2 - 4m_\pi^2}} \left(\frac{\alpha}{g_\omega} \right)^2 (g_{\sigma\pi\pi} m_\pi)^2 \frac{m_\omega^4}{(q^2 - m_\omega^2)^2 + m_\omega^2 \Gamma_\omega^{tot2}} F^2(q^2) \\ & \times |G_\sigma(q^2)|^2 [\Pi^0(q^2, q_z)]^2. \end{aligned} \quad (36)$$

The width Γ_ω^{tot} entering in Eq. (36) is the sum of $\Gamma_{\omega\rightarrow\pi\pi}$ given by Eq. (33) and of the ω width in free space, Γ_ω^{free} . This expression includes therefore the in-medium broadening of the ω -meson discussed in 4.1.

To evaluate the importance of such a process in heavy ion collisions, we compare the cross section for $\pi^+\pi^-$ annihilation in s-wave [Eq.(36) for charged pions] to the corresponding cross section for $\pi^+\pi^-$ annihilation in p-wave. The latter reaction is known to be the dominant source of e^+e^- pairs in relativistic heavy ion collisions ($1 < E/A < 2$ GeV) in the invariant mass region around the ρ - and ω -meson mass, $0.6 < m_{e^+e^-} < 0.8$ GeV [26–29]. Its cross section in the ρ -dominance model is given by [25]

$$\sigma_{\pi^+\pi^-\rightarrow e^+e^-}^{p-wave} = \frac{4\pi}{3} \left(\frac{\alpha^2}{q^2} \right) \sqrt{\frac{q^2 - 4m_\pi^2}{q^2}} \frac{m_\rho^4}{(q^2 - m_\rho^2)^2 + m_\rho^2 \Gamma_\rho^2}. \quad (37)$$

We calculate $\sigma_{\pi^+\pi^-\rightarrow e^+e^-}^{s-wave}$ and $\sigma_{\pi^+\pi^-\rightarrow e^+e^-}^{p-wave}$ at $\rho = 2\rho_0$ and $T=50$ MeV, i.e. under conditions which characterize the interaction region in central heavy ion collisions at relativistic energies. The cross section for $\pi^+\pi^-$ annihilation in s-wave will depend not only on q^2 but also on q_z . We compute it for $q_z=0.25$ GeV/c and $q_z=0.5$ GeV/c, to see the effect of the kinematics of

the ω -meson on the s-wave $\pi^+\pi^-$ annihilation cross section. For a proper comparison with the p-wave $\pi^+\pi^-$ annihilation cross section, we would need a consistent calculation of the ρ -meson width at $\rho = 2\rho_0$ and $T=50$ MeV. In the absence of such calculation and as the ρ -meson is expected to broaden substantially at high density [8,30], we use both the free width (Γ_ρ^{free}) and twice the free width in the evaluation of Eq. (37). The result is shown in Fig. 8. It is clear that the total cross section for $\pi^+\pi^-$ annihilation in p-wave is larger than the total cross section for $\pi^+\pi^-$ annihilation in s-wave in all cases.

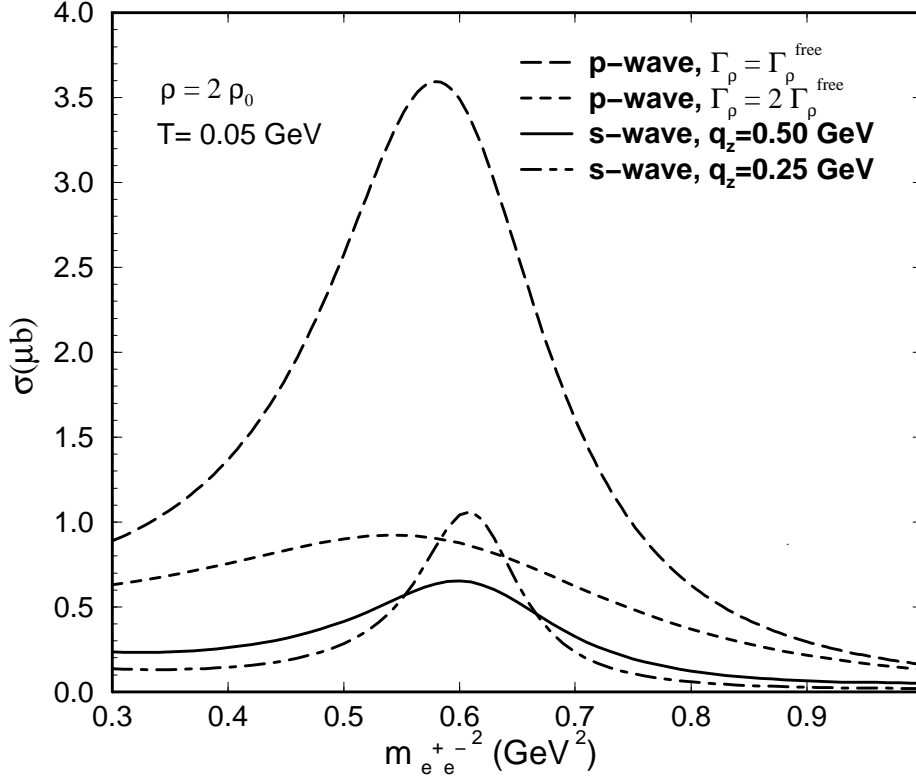


Fig. 8. P-wave and s-wave $\pi^+\pi^-$ annihilation cross sections into e^+e^- pairs. The long- and short-dashed lines show the p-wave annihilation cross section [Eq. (37)] calculated with $\Gamma_\rho = \Gamma_\rho^{free}$ and $\Gamma_\rho = 2\Gamma_\rho^{free}$ respectively. The full and dot-dashed lines show the s-wave annihilation cross section [Eq. (34)] for $q_z=0.5$ GeV/c and $q_z=0.25$ GeV/c.

To observe the momentum-dependent broadening of the ω -meson discussed in Subsection 4.1, kinematic cuts in the momentum of e^+e^- pairs produced in relativistic heavy ion collisions would be most helpful. At low momenta, the in-medium ω -meson width will be smaller and more likely to produce a structure in the e^+e^- spectrum, in particular if the ρ -meson is very broad. However, this structure is expected to reflect the direct production of ω -mesons in pion-nucleon and nucleon-nucleon collisions [26–29] rather than the s-wave $\pi^+\pi^-$ annihilation into e^+e^- pairs. Consequently, we do not anticipate that the observation of the latter process will be possible.

5. Conclusion

In this paper, we explore two consequences of a large nondiagonal $\omega\sigma$ polarization in matter at zero and finite temperature. Our most important result is a substantial broadening of ω -mesons moving with respect to a nuclear medium. The additional width, arising from the conversion of ω -mesons into σ -mesons through particle-hole excitations and the subsequent decay of the σ into two pions, can be much larger than the free width. At $T=0$, this in-medium width increases with density and with the 3-momentum of the ω -meson for $q \lesssim 0.5$ GeV/c. The effect decreases with increasing temperature in the Walecka Model. Our results are therefore most relevant for the studies of the propagation of ω -mesons in nuclei. In particular, the in-medium broadening of the ω meson should have observable consequences in experiments where ω -mesons are produced in heavy nuclear targets and observed in the e^+e^- decay channel [5,6]. As already emphasized, collisional broadening from the $\omega N \rightarrow \pi N$ and $\omega N \rightarrow \rho N$ reactions is expected to lead to a substantial further increase of the ω width in matter. All these processes should be included consistently in a calculation of the ω propagator at finite baryon density.

Our study of the inverse process, the s-wave $\pi\pi$ annihilation producing an ω -meson which can decay into an e^+e^- pair, shows that its contribution to dilepton spectra in relativistic heavy-ion collisions is much smaller than that of p-wave $\pi^+\pi^-$ annihilation in the ρ -channel. Consequently, we do not expect observable effects of this process in the total dilepton mass spectrum. However, the momentum dependent broadening of the ω meson may lead to a detectable effect also in heavy-ion collisions, once momentum cuts are applied.

Acknowledgements

Two of us (M. S. and Gy. W.) gratefully acknowledge the hospitality of GSI where much of this work was done. Gy. W. was supported in part by the Hungarian Research Foundation OTKA (grants T022931 and T016594) and by the french MAE/CEA 1996 Convention.

References

- [1] G.E. Brown and W. Weise, Phys. Rep. 22 (1975) 279.
- [2] L.S. Celenza, A. Pantziris and C.M. Shakin, Phys. Rev. C45 (1992) 205.
- [3] H.-C. Jean, J. Piekarewicz and A. G. Williams, Phys. Rev. C49 (1994) 1981.
- [4] G.E. Brown and M. Rho, Phys. Rev. Lett. 66 (1991) 2720.
- [5] CEBAF Proposal PR 89-001, Nuclear mass dependence of vector mesons using the photoproduction of lepton pairs, Spokesmen: D. Heddle and B.M. Freedom; CEBAF Proposal PR 94-002, Photoproduction of vector mesons off nuclei, Spokesmen: P.-Y. Bertin, M. Kossov and B.M. Freedom.
- [6] HADES Proposal (GSI Internal Report) and private communication.
- [7] Review of Particle Properties, Phys. Rev. D54 (1996) 1.
- [8] F. Klingl, N. Kaiser and W. Weise, Nucl. Phys. A624 (1997) 527.
- [9] H. Karami et al, Nucl. Phys. B154 (1979) 503; J. S. Danbury et al, Phys. Rev. D2 (1970) 2564.
- [10] B. Friman, in Proceedings of the APCTP Workshop on Astro-Hadron Physics, Seoul, Korea, October 25th-31st, 1997, nucl-th/9801053.
- [11] A. Weldon, Phys. Lett. B274 (1992) 133.
- [12] T. Kunihiro, Prog. Theor. Phys. Suppl. 120 (1995) 75.
- [13] P. A. Henning and B. L. Friman, Nucl. Phys. A490 (1988) 689.
- [14] K. Lim and C. J. Horowitz, Nucl. Phys. A501 (1989) 729.
- [15] J.W. Durso, A.D. Jackson and B.J. VerWest, Nucl. Phys. A345 (1980) 471.
- [16] B.D. Serot and J. D. Walecka, Adv. Nucl. Phys. 16 (1986) 1.
- [17] R. Machleidt, Adv. Nucl. Phys. 19 (1989) 189.
- [18] U.G. Meissner, Phys. Rep. 161 (1988) 213.
- [19] J. Boguta and A. R. Bodmer, Nucl. Phys. A292 (1977) 413.
- [20] C. Mahaux et al, Phys. Rep. 120 (1985) 1; G.E. Brown, J.H. Gunn and P. Gould, Nucl. Phys. 46 (1963) 598.
- [21] G. Janssen et al, Phys. Rev. D52 (1995) 2690.
- [22] W. Pauli and F. Villars, Rev. Mod. Phys. 21 (1949) 434.
- [23] C. Itzykson and J.-B. Zuber, Quantum Field Theory, McGraw-Hill, 1980.
- [24] N.M. Kroll, T.D. Lee and B. Zumino, Phys. Rev. 157 (1967) 1376.
- [25] C. Gale and J. Kapusta, Phys. Rev. C35 (1987) 2107.

- [26] E.L. Bratkovskaya et al., Phys. Lett. B 376 (1996) 12.
- [27] Gy. Wolf, Acta Phys. Pol. B26 (1995) 583.
- [28] Gy. Wolf, W. Cassing and U. Mosel, Nucl. Phys. A 552 (1993) 549.
- [29] Gy. Wolf et al, Nucl. Phys. A517 (1990) 615.
- [30] W. Peters et al, Nucl. Phys. A632 (1998) 109.